DYNAMIC SOIL RESPONSE FOR STRONG EARTHQUAKES: A SIMPLIFIED NON LINEAR CONSTITUTIVE MODEL

Luca LENTI[1], Jean-François SEMBLAT[2], Nicolas DELEPINE[3], Guy BONNET[4]

[1] PhD, Laboratoire Central des Ponts et Chaussées, Paris, France, Email: lenti@lcpc.fr
[2] Senior scientist, Laboratoire Central des Ponts et Chaussées, Paris, France, Email: semblat@lcpc.fr
[3] PhD, Laboratoire Central des Ponts et Chaussées, Paris, France, Email: delepine@lcpc.fr
[4] Professor, Laboratoire de Mécanique, Marne-la-Vallée, France, Email: bonnet@univ-mlv.fr

ABSTRACT

The seismic soil response can be analyzed in the frequency (linear or equivalent linear approaches) as well as in the time domain (e.g. complex constitutive models).
The nonlinear constitutive properties of soils being difficult and costly to determine, the present work proposes a simplified constitutive model to analyze the dynamic soil response for moderate or strong earthquakes at large scales (alluvial basins).
In this work, we consider a non linear viscoelastic constitutive model involving both non linear elasticity as well as non linear viscous behavior. The non linear elastic part of the model is described by a hyperbolic law. The description of the viscosity starts from a *Nearly Constant Quality Factor (NCQ)* model able to fulfil the causality principle for seismic wave propagating in dissipative materials. In the NCQ model, we introduced a dependence on the excitation level in order to consider the variations of moduli and the increasing damping ratio. This dependence is controlled during the 3D stress-strain path by the variation of the second order invariant of the strain tensor. Applications are performed to study the rheological response of the materials without considering wave propagation, and then to study the effects of nonlinearity on the generation of higher harmonics and shift of spectral frequencies during wave propagation in a sedimentary layer. Starting from the here proposed mechanical formulation including the main features of soil nonlinear behavior, the analysis of the nonlinear response of a sedimentary layer submitted by a vertical SH wave is then performed thanks to a discretization by the finite element method. Validations of the model for different inputs show its ability to recover low amplitude ground motion response. For larger excitation levels, the analysis of wave propagation in sedimentary layer leads to interesting results: at the free-surface the spectral peaks are shifted to lower frequency values (when compared to the input motion); higher frequency components are not overdamped as for the equivalent linear model; the amplification level is generally lower. These results show the ability of this simplified nonlinear model to investigate, in the near future, site effects in 2D/3D alluvial deposits for strong earthquakes.

Keywords: site effects, amplification, strong motion, nonlinear behavior, viscoelasticity

1. INTRODUCTION

The analysis of seismic wave propagation in alluvial basins is a difficult task since various phenomena are involved at different scales: resonance at the scale of the whole basin (Bard & Bouchon, 1985, Semblat et al., 2003), surface waves generation at the basin edges (Bard & Riepl-Thomas, 2000), soil non linear behaviour at the geotechnical scale (Iai et al., 1995, Bonilla et al., 2005). In this work, the attention is focused on the aspects of nonlinear behaviour of dry isotropic soils submitted to dynamic loadings. Various approaches are possible to model the dependence of the mechanical features of soils on the excitation level: equivalent linear model (Schnabel et al., 1972) improved by Kausel & Assimaki (2002) and nonlinear cyclic constitutive equations (e.g. based on plasticity) (Matasovic and Vucetic, 1995). The use of elastoplastic models is generally limited for large scale propagation analyses as a consequence of the large number of parameters needed. In this paper, a 3D nonlinear viscoelastic modelling of the dynamic soil behaviour is proposed. This model takes simultaneously into account nonlinear elasticity and viscosity.

2. MECHANICAL FORMULATION OF THE MODEL

2.1 3D linear viscoelasticity

2.1.1 General formulation

The 3D formulation of the viscoelastic model starts from the following relation

$$\sigma_{ij}=s_{ij}+p\delta_{ij} \tag{1}$$

where σ_{ij}, s_{ij}, δ_{ij} are the components of the Cauchy stress tensor, of the deviatoric stress tensor, and of the Kronecker unit tensor respectively and p the volumetric tension. For an isotropic material, we can write

$$p=K\cdot e_{kk} \tag{2}$$

where K and e_{kk} are the bulk modulus and the volumetric strain respectively. The relation between the components of the deviatoric stress tensor $\boldsymbol{s}$ and the shear deviatoric strain tensor $\boldsymbol{e}$ in the case of linear viscoelasticity is formulated in the frequency domain as simply as:

$$s_{ij}(\omega)=2M(\omega)e_{ij}(\omega) \tag{3}$$

$s_{ij}(\omega)$, $e_{ij}(\omega)$ are the Fourier transforms of the components of the deviatoric stress and strain tensors. $M(\omega)$ is the complex-valued, frequency-dependent, viscoelastic modulus from which we can define the specific attenuation Q^{-1} in the following way :

$$2\xi=Q^{-1}(\omega)\approx Im(M(\omega))/Re(M(\omega)) \tag{4}$$

where ξ is the damping ratio and Re and Im are the real and imaginary parts of a complex variable (resp.).

2.1.2 NCQ models

This family of models is defined in term of the quality factor Q. A nearly constant Q in a broad frequency range has been derived by many authors by various combinations of dashpot and spring elements describing different rheological cells (Biot (1953), Liu et al. (1976), Mozco & Kristek (2005), etc.). Hereafter the implementation of the *NCQ* model of Emmerich & Korn (1987), principally based on the generalized Maxwell model, is briefly presented to recall its essential features. In the following, this model will be generalized in order to make the attenuation dependent on the strain level. In the linear case, a frequency dependent complex modulus can be defined as follow (variables with bracket are not tensorial):

$$M(\omega)=M_U\left(1-\frac{\sum_{l=1}^{n} y_{(l,0)}\omega_{(l)}/(i\omega+\omega_{(l)})}{1+\sum_{l=1}^{n} y_{(l,0)}}\right) \tag{5}$$

M_U is the unrelaxed (instantaneous) modulus and M_R is the relaxed (long term) modulus. The $y_{(l,0)}$ variables characterize the rheological model and are calculated by means of an optimization method in order to obtain a nearly constant attenuation in a certain frequency range. Using the eqs. (4) and (5) the attenuation has the following expression:

$$Q^{-1}(\omega)=\frac{\mathrm{Im}\,M(\omega)}{\mathrm{Re}\,M(\omega)}=\frac{\sum_{l=1}^{n} y_{l,(0)}\dfrac{\omega/\omega_l}{1+(\omega/\omega_l)^2}}{1+\sum_{l=1}^{n} y_{l,(0)}\dfrac{(\omega/\omega_l)^2}{1+(\omega/\omega_l)^2}} \tag{6}$$

The $\omega_{(l)}$ frequencies characterize each individual rheological cell. The constitutive equations of the linear viscoelastic model are then found:

$$s_{ij}(t)=2M_U\left[e_{ij}(t)-\sum_{l=1}^{n}\zeta_{(l)}(t)\right] \tag{7}$$

and

$$\dot{\zeta}_{(l)}(t)+\omega_{(l)}\zeta_{(l)}(t)=\omega_{(l)}\frac{y_{(l,0)}}{1+\sum_{l=1}^{n}y_{(l,0)}}e_{ij}(t) \tag{8}$$

where $\zeta_{(l)}(t)$ are relaxation parameters physically related to the anelastic deformation of the l^{th}-cell.

2.2 3D nonlinear viscoelastic model

2.2.1 Principles of the nonlinear model

In order to describe the shear modulus and damping variations of the soils vs the excitation level, an elastic potential function and a dissipation function depending on the second invariant of the strain tensor are introduced. In particular the "NCQ" model, already described above, now becomes able to consider increasing damping ratios as suggested from earthquakes records and geotechnical data (Iai et al, 1995; Vucetic, 1990). The changing of the attenuation vs induced strain level is controlled during the 3D stress-strain path by the variation of the second order invariant of the strain tensor.

2.2.2 Formulation of the extended NCQ model (e-NCQ)

To account for the nonlinear behaviour of soils in the case of any 3D stress-strain path, equation (7) is generalized as follows:

$$s_{ij}(t)=2M_U(J_2)\left[e_{ij}(t)-\sum_{l=1}^{n}\zeta_{(l)}(t,y_{(l)}(J_2))\right] \tag{9}$$

where J_2 is the second invariant of the deviatoric strain tensor.
In addition, the shear modulus is assumed to change during the global stress-strain path according to the following relation:

$$M_U(J_2)=M_{U,0}\left[1-\Phi(J_2)\right] \tag{10}$$

with

$$\Phi(J_2)=\frac{\alpha|J_2|^{\frac{1}{2}}}{1+\alpha|J_2|^{\frac{1}{2}}} \tag{11}$$

and where $M_{U,0}$ denotes the unrelaxed modulus characterizing the instantaneous response of the soil at small strains and α is a parameter quantifying its nonlinear behaviour for larger strains. The octahedral strain γ_{oct} is now introduced:

$$|\gamma_{oct}|=2|J_2|^{\frac{1}{2}} \tag{12}$$

It leads to

$$M_U(|\gamma_{oct}|)=M_{U,0}\left[1-\Phi(|\gamma_{oct}|)\right] \tag{13}$$

where:

$$\Phi(|\gamma_{oct}|)=\frac{\alpha|\gamma_{oct}|/2}{1+\alpha|\gamma_{oct}|/2} \tag{14}$$

Such a dependence of the nonlinear elastic modulus on the octahedral strain implies a strain dependence for the variables $y_{(l)}$ and $\zeta_{(l)}$. In the case of 3D loadings, different authors (El Hosri, 1984; Bonnet et Heitz; 2005) proposed relations making ξ depend on the strain level.

Here we adopt the following one:

$$\xi(|\gamma_{\rm oct}|) = \xi_0 + (\xi_{\max} - \xi_0)\Phi(|\gamma_{\rm oct}|) \tag{15}$$

where ξ_0 and ξ_{max} characterize the dissipated energy in the small and larger strain ranges respectively. Typical $M_U(\gamma)$=G(γ) and $\xi(\gamma)$ curves are reported in Fig. 2. The ξ and Q^{-1} parameters are related by:

$$Q^{-1} = 2\xi(|\gamma_{oct}|) \tag{16}$$

2.2.3 Features of the extended NCQ model

In the previous paragraph, the solution of equation (9) in the limit of low excitation levels has been found. For low octahedral strain, we may consider that:

$$Q_0^{-1} = 2\xi_0 \tag{17}$$

and

$$M_U(|\gamma_{oct}| \approx 0) = M_{U,0} = G_0 \tag{18}$$

For every other value of the induced strain, the Q^{-1} factor increases with strain according to equation (16). This change has no influence on the frequency range in which Q^{-1} is constant. In other words, in equation (8) only the variables $y_{(l,0)}$ change to account for the variation of the damping with strain. We therefore introduce a strain variation of the variables $y_{(l)}$ in the following form:

$$y_{(l)}(|\gamma_{oct}|) = c(|\gamma_{oct}|)\, y_{(l,0)} \tag{19}$$

Using equations (4), (12) and (14), for every level of induced octahedral strain, equations (5) and (6) can be rewritten in the following form, respectively:

$$M(\omega,|\gamma_{oct}|) = M_U(|\gamma_{oct}|)\left(1 - \frac{c(|\gamma_{oct}|)\sum_{l=1}^{n} y_{(l,0)}\omega_l/(i\omega + \omega_{(l)})}{1 + c(|\gamma_{oct}|)\sum_{l=1}^{n} y_{(l,0)}}\right) \tag{20}$$

$$Q^{-1}(\omega,|\gamma_{oct}|) \approx c(|\gamma_{oct}|)\sum_{l=1}^{n} y_{(l,0)} \frac{\omega/\omega_{(l)}}{1 + (\omega/\omega_{(l)})^2} \tag{21}$$

where, using equation (15), $c(|\gamma_{oct}|)$ is given by:

$$c(|\gamma_{oct}|) = \frac{Q^{-1}(\omega,|\gamma_{oct}|)}{Q_0^{-1}} = \frac{\xi(|\gamma_{oct}|)}{\xi_0} = \left[1 + \frac{\xi_{\max} - \xi_0}{\xi_0}\Phi(|\gamma_{oct}|)\right] \tag{22}$$

For every level of induced octahedral strain, equation (8) can be written in a more general form:

$$\dot{\zeta}_l(t) + \omega_l \zeta_l(t) = \omega_j \frac{c(|\gamma_{oct}|)\, y_{l,0}}{1 + c(|\gamma_{oct}|)\sum_{l=1}^{n} y_{l,0}} e_{ij}(t) \tag{23}$$

The latter expression and equation (13) are used to solve equation (9) in the time domain.

2.3 Synthesis: 1D case

For a unidirectional propagating shear wave, $|\gamma_{oct}|$ is equal to $2|\gamma|$, where γ is the shear strain. Equation (13) can be written in the form:

$$M_U(|\gamma|) = G(|\gamma|) = \frac{G_0}{1+\alpha|\gamma|} \tag{24}$$

In this case, equation (24) expresses a hyperbolic law for the reduction of the shear modulus as the one proposed by Hardin and Drnevich (1972). As a consequence, the following equation for the function $c(|\gamma_{oct}|)$ is obtained:

$$c(|\gamma|) = \left[1 + \frac{\xi_{\max} - \xi_0}{\xi_0}\left(\frac{\alpha|\gamma|}{1+\alpha|\gamma|}\right)\right] \tag{25}$$

where ξ_{max} and ξ_0 are two constant rheological experimental values. At every time, the values associated to the functions $\zeta_{(l)}(t)$ are obtained by solving the following equations:

$$\dot{\zeta}_{(l)}(t) + \omega_{(l)}\zeta_{(l)}(t) = \omega_{(l)} \frac{c(|\gamma|)\, y_{(l,0)}}{1 + c(|\gamma|)\sum_{l=1}^{n} y_{(l,0)}} e(t) \tag{26}$$

where the variables $y_{(l,0)}$ are known for the lower strain Q^{-1} value (formula (6)). Finally, the rheological equation (9) is used for the considered 1D case:

$$s(t) = \frac{2G_0}{1+\alpha|\gamma|}\left[e(t) - \sum_{l=1}^{n} \zeta_l(t, y_l(\gamma))\right] \tag{27}$$

3. VALIDATION OF THE CONSTITUTIVE MODEL FOR CYCLIC LOADINGS

The nonlinear constitutive law is firstly validated for 1D cyclic loadings of variable amplitudes directly solving eqs (25), (26) and (27) without considering wave propagation. The α parameter is α=1000 and the elastic shear modulus G_0=80MPa. We consider eqs (25) and (26) with the following asymptotic damping values: ξ_0=0.025 and $\xi_{\max}$=0.25.

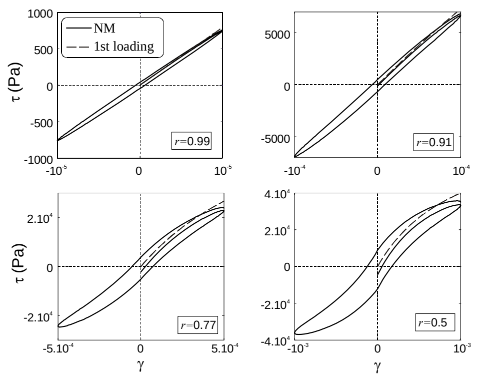

Figure 1: stress-strain curves from cyclic loadings of variable maximum amplitudes at 10Hz: nonlinear extended NCQ model (solid) and 1st loading curve.

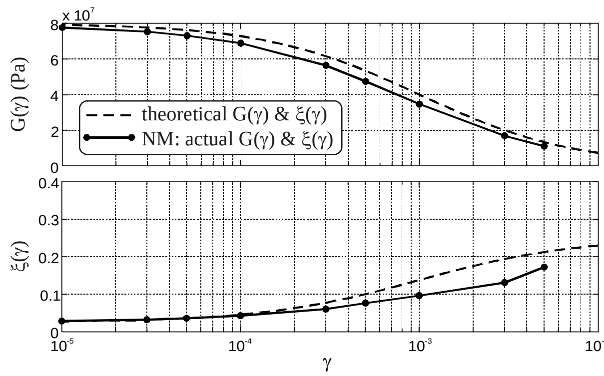

Figure 2: comparison of the shear modulus and damping values of the extended NCQ model (cyclic loadings) with the theoretical variations predicted by equations (14) and (25).

In Fig. 1, some of the results (at 10Hz) are displayed as stress-strain loops for $\gamma_{\max}$=10^{-5}, 10^{-4}, 5.10^{-4}. For each case, the secant shear modulus G is calculated and normalized by G_0 (the ratio r=G/G_0 is given in each curve). The first case (Fig. 1, top left), corresponding to $\gamma_{\max}$=10^{-5} and r=0.99, leads to a nearly linear response with an elliptical stress-strain loop. In the 2nd case, $\gamma_{\max}=10^{-4}$ and $r=0.91$ (Fig. 1, top right), the area of the loop is larger and there is a slight decrease of the shear modulus. For the largest excitations ($\gamma_{\max}=5.10^{-4}$; $r=0.77$) and ($\gamma_{\max}=10^{-3}$; $r=0.50$) (Fig. 1, bottom), the nonlinear effects are obvious since the stress-strain loops are strongly modified (secant modulus, area, etc). From these loops, it is straightforward to derive the secant shear modulus as a function of maximum shear strain. For each loading level the dissipation has been quantified as well (Kramer, 1996). The actual $G(\gamma_{\max})$ and $\xi(\gamma_{\max})$ curves are then compared to the theoretical curves in Fig. 2. The effective shear modulus (solid) is very close to the theoretical one (dotted). For the damping ratio, the difference is larger for large shear strains, but the effective dissipation increases as expected.

4. NUMERICAL IMPLEMENTATION FOR WAVE PROPAGATION

4.1. Theory

The mechanical model described above is introduced into the framework of the finite element method, for the case of a unidirectional shear loading. We consider a homogeneous layer with nonlinear behavior over an elastic bedrock. The domain is discretized into $(N-1)/2$ linear quadratic finite elements, each of the N nodes having 1 degree of freedom (horizontal motion) (Fig. 3). Using square brackets […] and braces {…} to denote matrices and vectors, the discretized equation of motion can be written in the following form at each time step $(n+1)\Delta t$:

$$\begin{cases} [M]\{a_{n+1}\} + [C]\{v_{n+1}\} + [K(u_{n+1})]\{u_{n+1}\} = \{F_{n+1}\} \\ \dot{\zeta}_{(l)}(t) + \omega_{(l)}\zeta_{(l)}(t) = H_{(l)}(\mathrm{u}_{\mathrm{n+1}}) \quad ; \quad l = 1, l_{\max} \end{cases} \tag{28}$$

where $[M]$, $[C]$ and $[K(u_{n+1})]$ represent the mass, the radiation condition at the bedrock/layer interface (elastic substratum), and the stiffness matrix respectively. $\{a_{n+1}\}$, $\{v_{n+1}\}$ and $\{u_{n+1}\}$ are the acceleration, velocity and displacement vector respectively, while $\{F_{n+1}\}$ is the vector of external forces at the interface. $\zeta_{(l)}$ and $\omega_{(l)}$ are the relaxation parameters and central frequencies of the rheological cells (resp.), $H_{(l)}(\mathrm{u}_{n+1})$ corresponds to the right hand-side term in equation (26) and l_{max} is the total number of cells included in the model (l_{max}=3 herein).
For the time integration, an extension of the Newmark formulation is used, namely an unconditionally stable implicit α-HHT scheme (Hughes, 1987). This scheme allows a control of the higher frequencies generated during the propagation. At each time step, the Newton-Raphson iterative algorithm is adopted to deal with the nonlinear nature of the first equation in system (28). The Crank-Nicolson procedure (Zienkewicz, 2005) is simultaneously used in order to estimate the $\zeta_{(l)}(t)$ variables in the first order differential equations (system (28), bottom).

4.2. Applications to the amplification of synthetic wavelets

We performed two different types of simulations: linear model (LM) and nonlinear model (NM). For the first one ($\beta_0 = \beta_{max} = 2.5\%$ and $\alpha = 0$), mechanical and dissipative properties of the material do not depend on the excitation level while, in the second case ($\beta_0 = 2.5\%$, $\beta_{max} = 25\%$ and $\alpha = 1000$), both elastic and dissipative properties are function of the induced strain as depicted in Fig. 4. For this model, we performed simulations for a 30m thick soil layer on elastic bedrock without any seismic impedance contrast. The input has been constructed making the product in the time domain between 2 sinusoids whose frequencies are respectively 3Hz and 0.33Hz. The total duration of the resulting acceleration signal is about 2 s and its maximum amplitude is multiplied by a weighting coefficient every time. The comparisons between the LM (dotted line) and the NM (solid line) are made in Fig. 5 in terms of acceleration time histories and Fourier spectra at the top of the layer for 3 input acceleration levels (0.5, 1.0 and 1.5 m/s^2). For all the signals at the free surface, the amplification by a factor 2 has been taken into account. In Fig. 6, the results at the centre of the soil layer are shown, in particular the outputs in terms of stress time histories and stress-strain paths for various excitation levels given previously. The NM time graphs of Figs. 5 and 6 show a time delay in the propagation with respect to the corresponding graphs of the LM results. This time delay becomes larger when the excitation level increases. For the NM case, the frequency content of the calculated accelerations generally shows two features which should be mentioned (Fig. 5) : 1) a significant decrease of the spectral amplitude for the dominating frequency of the input signal with

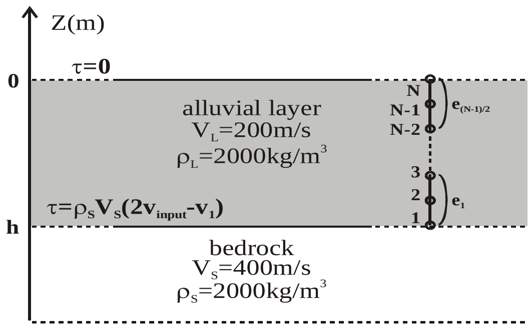

Figure 3: 1D soil layer over an elastic bedrock: finite element discretization and absorbing boundary condition at the interface.

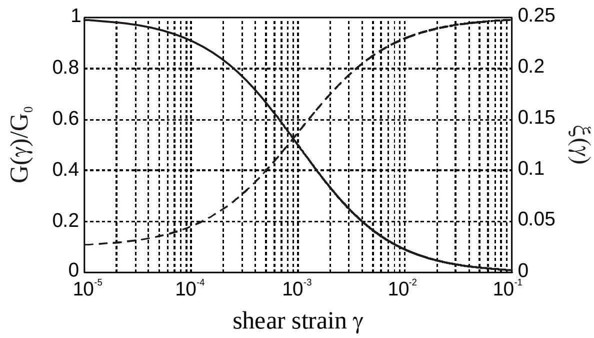

Figure 4 : modulus reduction (solid) and increasing damping (dashed) vs shear strain.

increasing excitation level; 2) increasing of 3rd and 5th (Van Den Abeele et al., 2000). The stress-strain paths show a significant energy dissipation increase and a strong reduction of the shear modulus (Fig. 6).

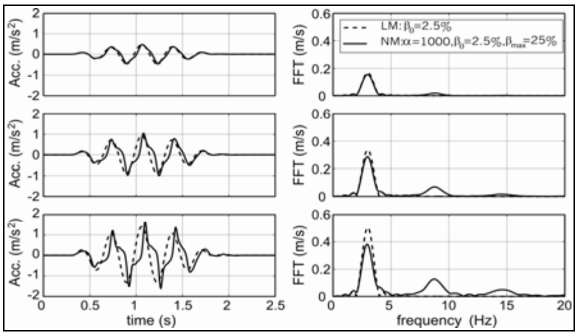

Fig. 5: accelerations (left) and corresponding Fourier spectra (right) at the top of the soil layer in the homogeneous case, for 3 values of the input maximum acceleration on bedrock (0.5, 1.0 and 1.5 m/s^2), and in the case of linear and nonlinear simulations (LM and NM).

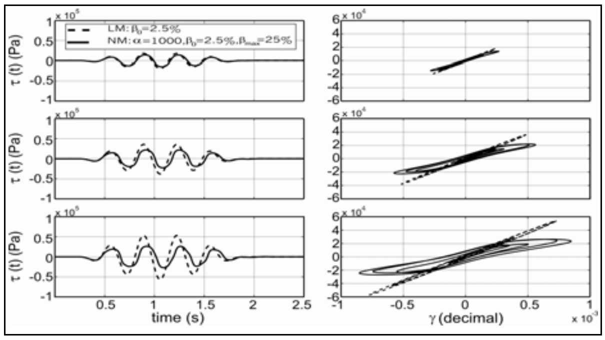

Fig. 6 : stress time histories (left) and stress-strain paths (right) in the middle of the soil layer, in the homogeneous case, for 3 values of the input maximum acceleration on bedrock (0.5, 1.0 and 1.5 m/s2), and in the case of linear and nonlinear simulations (LM and NM).

5. CONCLUSIONS

A 3D nonlinear viscoelastic model ("extended NCQ" or *e-NCQ*) is proposed to approximate the hysteretic behaviour of alluvial deposits undergoing dynamic excitations. Such nonlinear features as the reduction of shear modulus and the increase of damping are controlled by the variations of the 2nd invariant of the strain tensor during multidimensional loadings. In the case of a unidirectional shear loading, nonlinearity is controlled by only one shear strain component: the nonlinear elasticity by a hyperbolic law and the viscosity by a *NCQ* model in the frequency domain but strain amplitude dependent. In 1D nonlinear wave propagation simulations, the model allows to account for both the generation of higher order harmonics, the reduction of the spectral amplitudes and a decreasing of outputs spectral frequencies for increasing amplitudes of inputs. The interest of the simplified nonlinear model proposed herein is to reduce the computational cost for the analysis of strong seismic motion in 2D/3D alluvial basins. In fact, in the 1D case, the reduction of shear modulus is controlled by a hyperbolic law with only one parameter α estimated from the experimental knowledge of the $G(\gamma)$ curve. As a consequence, the dissipation properties are directly derived from the hyperbolic law and from two other characteristic parameters responsible for the minimum and maximum loss of energy at lower and larger strain levels, ξ_0 and ξ_{max}. These are sufficient to give an overall description of the unloading and reloading phases during the seismic sequence. The proposed model will allow future computations in the case of 2D or either 3D alluvial basins for which the amplification is generally found to be much larger than predicted through 1D analyses (Chaillat et al., 2008; Sánchez-Sesma & Luzón, 1995, Semblat 2000).

REFERENCES

Bard, P-Y. and Bouchon, M. (1985). The two dimensional resonance of sediment filled valleys, Bull. Seism. Soc. Am., vol. 75, pp. 519-541.

Bard P.Y. and Riepl-Thomas J. (2000). Wave propagation in complex geological structures and their effects on strong ground motion, Wave motion in earthquake eng., Kausel & Manolis eds, WIT Press, Southampton, Boston, pp.37-95.

Biot M.A. (1958). “Linear thermodynamics and the mechanics of solids”, Proc. 3rd U.S. Nat. Conf. of Appl. Mech., ASME, New-York, N.Y., pp. 1-18.

Bonilla L.F., Archuleta R.J., Lavallée D. (2005). “Hysteretic and Dilatant Behavior of Cohesionless Soils and Their Effects on nonlinear Site Response : Field Data Observations and Modeling” *Bulletin of the Seismological Society of America*, vol. 95, No 6, pp. 2373-2395.

Bonnet G. and Heitz J.F. (2005). “Nonlinear seismic response of a soft layer. In: G. Duma Editor”, *Proceeding 10th European Conference on Earthquake Engineering* Balkema, Rotterdam, pp. 361-364.

Chaillat S., Bonnet M., Semblat J-F (2008). “A multi-level Fast Multipole BEM for 3-D elastodynamics in the frequency domain”, Computer Methods in Applied Mechanics and Engineering, doi:10.1016/j.cma.2008.04.024 (to appear).

El Hosri, M.S., Biarez, H., Hicher, P.Y. (1984). Liquefaction characteristics of silty clay. Proc. Eight World Conf. On Earthquake Eng. Prentice Hall, NJ, pp. 277–284.

Emmerich H. and Korn M. (1987). “Incorporation of attenuation into time-domain computations of seismic wave fields”, *Geophysics*, vol. 59, No 9, pp. 1252-1264.

Hardin B.O. and Drnevich, V.P. (1972). “Shear modulus and damping in soils: Design equations and curves.” Journal of Soil Mechanics and Foundation Engineering Division, ASCE, Vol. 98, No. 7, pp. 667-692.

Hughes T.J.R (1987). “The Finite Element Method – Linear Static and Dynamic Finite Element Analysis” *Prentice-Hall, Inc.*, New Jersey.

Iai S., Morita T., Kameoka T., Matsunaga Y., Abiko K. (1995). “Response of a dense sand deposit during 1993 Kushiro-Oki Earthquake”, *Soils Found.*, vol. 35, pp. 115-131.

Kausel E. and Assimaki D. (2002) “Seismic simulation of inelastic soils via frequency-dependent moduli and damping” *Journal of Engineering Mechanics*, vol. 128, No. 1: pp. 34–47.

Kramer S.L. (1996). “Geotechnical earthquake engineering”, 653 p., Prentice-Hall.

Liu H.P., Anderson D.L., Kanamori H. (1976). Velocity dispersion due to anelasticity: Implications for seismology and mantle composition. *Geophys. J. R. Astron. Soc.,* vol. 47, pp. 41-58.

Matasovic N. and Vucetic, M. (1995). “Seismic response of soil deposits composed of fully-saturated clay and sand layers” *Proceedings of the First International Conference on Earthquake Geotechnical Engineering,* JGS, 1, pp. 611-616, Tokyo, Japan.

Moczo P. and Kristek J. (2005). “On the rheological models used for time-domain methods of seismic wave propagation” *Geophys. Res. Lett.*, vol. 32, L01306.

Semblat J.F., Paolucci R., Duval A.M. (2003). “Simplified vibratory characterization of alluvial basins” *C.R. Geoscience*, 335.

Semblat J.F., Duval A.M., Dangla P. (2000). “Numerical analysis of seismic wave amplification in Nice (France) and comparisons with experiments”, *Soil Dynamics and Earthquake Eng.*, vol. 19, No. 5, pp. 347-362.

Schnabel P.B., Lysmer J., Seed H.B. (1972). “SHAKE-A computer program for equation response analysis of horizontally layered sites” *Rep. No. EERC 72-12,* University of California, Berkeley.

Van Den Abeele, K., P. A. Johnson, and A. Sutin, (2000). “Nonlinear Elastic Wave Spectroscopy (NEWS) techniques to discern material damage”. Part I: Nonlinear Wave Modulation Spectroscopy (NWMS). Res. Nondestr. Eval., vol. 12, No. 1, pp. 17-30,.

Vucetic M. (1990). “Normalized behaviour of clay under irregular cyclic loading” Can. Geotech. J., 27, 29 – 46.

Zienkewicz, O. C. and Taylor, R. L. (2005). "The Finite Element Method for Solid and Structural Mechanics," Elsevier, 6th edition, January 2005, pp.632